

Ab Initio Studies of Abstraction Reactions $\text{XH}_n + \text{H}_2 \rightarrow \text{XH}_{n+1} + \text{H}$ ($\text{X} = \text{C}, \text{N}, \text{Si}, \text{P}$)

Mark S. Gordon,*† David R. Gano,† and Jerry A. Boatz†

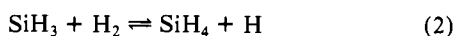
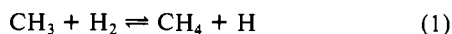
Contribution from the Departments of Chemistry, North Dakota State University, Fargo, North Dakota 58105, and Minot State College, Minot, North Dakota 58701. Received January 14, 1983

Abstract: The abstraction reactions $\text{CH}_3 + \text{H}_2 \rightarrow \text{CH}_4 + \text{H}$, $\text{SiH}_3 + \text{H}_2 \rightarrow \text{SiH}_4 + \text{H}$, $\text{NH}_2 + \text{H}_2 \rightarrow \text{NH}_3 + \text{H}$, and $\text{PH}_2 + \text{H}_2 \rightarrow \text{PH}_3 + \text{H}$ have been studied with a variety of methods, including MCSCF, POL-CI, UMP2, and UMP3. In agreement with the observed thermochemistry, abstraction by methyl radical is found to proceed more easily than by silyl, and the reverse of the last reaction occurs with a very small (~ 5.6 kcal/mol) barrier. POL-CI appears to be a consistently reliable approach for this type of reaction.

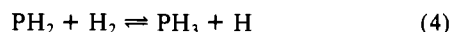
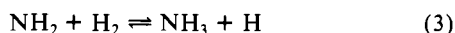
I. Introduction

Alkyl and silyl radicals are among the most common species generated in pyrolyses and photolyses of alkylsilanes.¹ Because these radicals are reactive intermediates, the final product distributions which result from unimolecular dissociations of alkylsilanes will be strongly influenced by the secondary reactions involving the primary products. One of the most likely secondary reactions involving alkyl or silyl radicals is abstraction of a hydrogen, and it is particularly of interest to establish the relative abstracting ability of alkyl vs. silyl radicals. From purely thermodynamic considerations one might predict the approximately 14 kcal/mol difference in CH vs. SiH bond energies to translate into a much slower rate of abstraction by silyl radicals. This is not necessarily the case, however, since the relative rates depend to a large degree on the details of the potential energy surfaces.

The present work includes a competitive study of the simplest abstraction reactions involving alkyl and silyl radicals,



as well as the corresponding reactions for ammonia and phosphine:



Because our intent is to study a large number of such reactions, it is important to establish an efficient yet reliable approach for obtaining at least internally consistent thermodynamic and kinetic information. To help evaluate the different methodologies used here, the well-studied linear $\text{H} + \text{H}_2$ reaction is included as well.

The most accurate calculation on the H_3 surface was carried out by Siegbahn and Liu³ with a large-scale CI and extended basis set. These authors find a barrier of 9.8 cal/mol. For the $\text{CH}_4 + \text{H}$ reaction, Walch⁴ finds a 15.9 kcal/mol barrier with use of POL-CI⁵ with an extended basis set. Recent summaries of the theoretical literature have been given by Klimo and Tino⁶ and Carskey, Hubac, and Staemmler⁷ for the $\text{H} + \text{H}_2$ and $\text{CH}_3 + \text{H}_2$ reactions, respectively.

II. Computational Methods

Five basis sets were used in this study. All structures were calculated with the split valence 3-21G basis set.⁸ The structural determinations were followed by single-point calculations using the 6-31G* basis set⁹ (denoted 6-31G* // 3-21G) with correlated wave functions. For the two test systems, H_3 and CH_5 , the larger 6-31G**⁹, 6-311G*,¹⁰ and 6-311G**¹⁰ basis sets were used. Transition states were detected by using the EMIN program developed by Hilderbrandt¹¹ connected to the HONDO¹² analytical gradient program.

Two approaches were used to obtain correlated wave functions. The first supplements unrestricted Hartree-Fock molecular orbitals with second- and third-order Rayleigh-Schrödinger Møller-Plesset perturba-

Table I. Structural Changes Relative to Separated Reactants and Products

molecule	% increase in $R(\text{XH}')^a$	% increase in $R(\text{H}'\text{H}'')$
H_3	27	27
CH_5	26	26
SiH_5	13	42
NH_4	23	32
PH_4	8	61

tion theory (UMP2 and UMP3¹³). These wave functions are obtained by using an IBM version of GAUSSIAN80.¹⁴ The second approach is to augment restricted Hartree-Fock wave functions with a small (3×3) MCSCF¹⁵ augmented by POL-CI.⁵ The latter is the method used by Walch⁴ in his study of reaction 1. In the generation of the POL-CI configurations the inner shells were frozen and, except for H_3 , the highest virtual orbital in each irreducible representation was excluded. For CH_5 and SiH_5 , the POL-CI involved 1207 SAAPS,¹⁵ while 1121 SAAPS were included in the NH_4 and PH_4 calculations.

III. Results and Discussion

A. Geometries. The 3-21G structures for all reactants and products have been published earlier.⁸ The transition-state geometries are summarized in Figure 1. For H_3 , CH_5 , and SiH_5 , the XHH angle was assumed to be linear, while only C_s symmetry was assumed for PH_4 and NH_4 . The H_3 transition-state geometry predicted by 3-21G is in good agreement with that of Siegbahn and Liu.³ The transition-state bond length seems to be insensitive to basis set and correlation effects, since 6-31G** SCF, UMP2,

(1) See, for example, D. J. Doyle, S. K. Tokach, M. S. Gordon, and R. D. Koob, *J. Phys. Chem.*, **86**, 3626 (1982).

(2) H. E. O'Neal and M. A. Ring, *J. Organomet. Chem.*, **213**, 419 (1981).

(3) P. Siegbahn and B. Liu, *J. Chem. Phys.*, **245** (1978).

(4) S. P. Walch, *J. Chem. Phys.*, **72**, 4932 (1980).

(5) P. J. Hay and T. H. Dunning, *J. Chem. Phys.*, **64**, 5077 (1976).

(6) V. Klimo and J. Tino, *Mol. Phys.*, **46**, 541 (1982).

(7) P. Carskey, I. Hubac, and V. Staemmler, *Theor. Chim. Acta*, **60**, 445 (1982).

(8) J. S. Binkley, J. A. Pople, and W. J. Hehre, *J. Am. Chem. Soc.*, **102**, 939 (1980). M. S. Gordon, J. S. Binkley, J. A. Pople, W. J. Pietro, and W. J. Hehre, *Ibid.*, **104**, 2797 (1982).

(9) P. C. Hariharan and J. A. Pople, *Theor. Chim. Acta*, **28**, 213 (1973); M. S. Gordon, *Chem. Phys. Lett.*, **76**, 163 (1980); M. M. Francl, W. J. Pietro, W. J. Hehre, J. S. Binkley, M. S. Gordon, D. J. DeFrees, and J. A. Pople, *J. Chem. Phys.*, **77**, 3654 (1977).

(10) R. Krishnan, J. S. Binkley, R. Seeger, and J. A. Pople, *J. Chem. Phys.*, **72**, 650 (1980).

(11) R. L. Hilderbrandt, *Comput. Chem.*, **1**, 179 (1977).

(12) H. F. King and M. Dupuis, *J. Comput. Phys.*, **21**, 144 (1976); M. Dupuis and H. F. King, *Int. J. Quantum Chem.*, **1**, 613 (1977).

(13) J. A. Pople, J. S. Binkley, and R. Seeger, *Int. J. Quantum Chem., Symp.*, **10**, 1 (1976).

(14) J. S. Binkley, R. A. Whiteside, R. Krishnan, R. Seeger, D. J. DeFrees, H. B. Schegel, S. Topiol, L. R. Kahn, and J. A. Pople, *Quantum Chemistry Program Exchange*, Indiana University, 1980.

(15) K. Ruedenberg, L. M. Cheung, and S. T. Elbert, *Int. J. Quantum Chem.*, **16**, 1069 (1979).

*North Dakota State University.

†Minot State College.

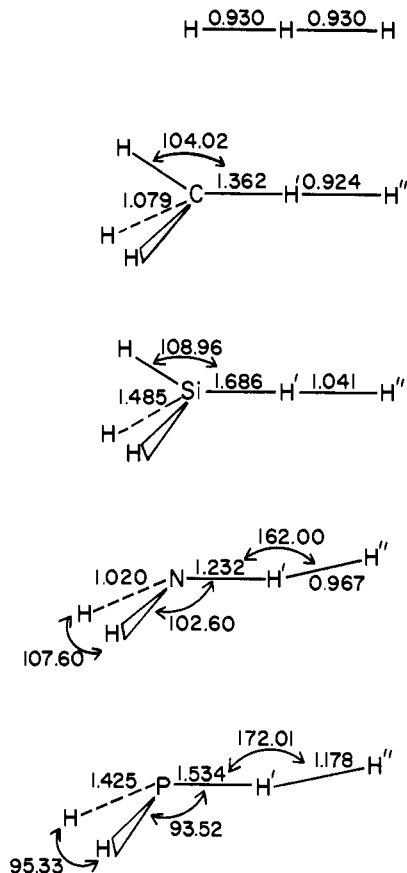


Figure 1. Transition-state structures. Bond lengths in angstroms, angles in degrees.

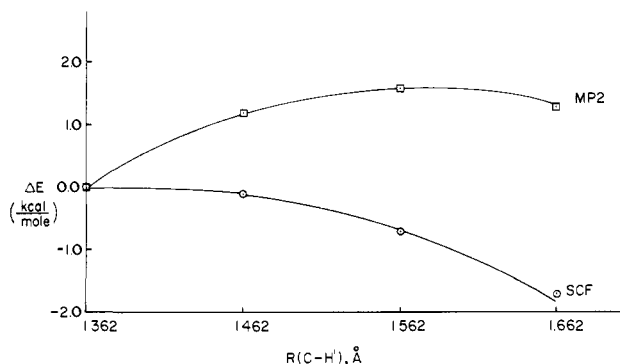


Figure 2. Variation of SCF and MP2 energies with C-H' bond length near the CH₃ transition state.

and UMP3 all predict a bond length between 0.92 and 0.93 Å.

Except for the C-H' distance, the predicted transition-state geometry for CH₃ is in good agreement with the POL-CI results of Walch.⁴ The C-H' bond length is found to be about 0.1 Å shorter than that predicted by POL-CI and about the same as that predicted by Botschwina and Meyer¹⁶ using PNO-CEPA wave functions. The range of values predicted for R(C-H') has been summarized recently by Schatz, Walch, and Wagner¹⁷ and is clearly due in part to the flatness of the surface in the region near the transition state. This is illustrated in Figure 2, where the energy relative to the transition-state bond length is plotted for 6-31G* SCF and MP2/6-31G* as a function of increasing distance. The HC...H' angle has been re-optimized at each point with all other parameters being held fixed. For both levels of calculation, the change in energy is less than 2 kcal/mol when

Table II. Barriers in the H + H₂ Reaction (kcal/mol)

basis set	RHF	UHF	UMP2	UMP3	MCSCF	POL-CI
6-31G	25.0	18.4	17.6	17.1	17.8	14.4
6-311G	24.2	16.9	16.2	15.5	16.9	13.2
6-31G**		18.4	15.8	15.1		
6-311G**		17.7	14.2	13.1		

Table III. Energetics in the CH₃ + H₂ $\xrightarrow{\Delta E_1}$ CH₅ $\xrightarrow{-\Delta E_2}$ CH₄ + H Reaction (kcal/mol)

basis set	RHF	UHF	UMP2	UMP3	MCSCF	POL-CI
A. ΔE_1 (Experiment = 10.9 kcal/mol ^a)						
6-31G*	25.1	20.6	14.2	15.7	19.0	9.9
6-311G*		20.6	13.7	15.1		
6-31G**		21.2	14.1	15.5		
6-311G**		21.6	13.1	14.3		
B. ΔE_2 (Experiment = 11-12 kcal/mol ^b)						
6-31G*	32.6	26.0	26.1	24.5	24.2	17.6
6-311G*		25.2	25.4	23.7		
6-31G**		24.9	23.1	21.5		
6-311G**		23.8	20.5	18.4		
C. $\Delta E = \Delta E_2 - \Delta E_1$ (Experiment = 2.6 kcal/mol ^b)						
6-31G*	7.5	5.4	11.9	8.8	5.2	7.7
6-311G*		4.6	11.7	8.6		
6-31G**		3.7	9.0	6.0		
6-311G**		2.2	7.4	4.1		

^a From J. S. Shapiro and R. E. Weston, *J. Phys. Chem.*, 76, 1669 (1972), uncorrected for zero-point effects. ^b See ref 4 of text.

the bond length is stretched by 0.3 Å.

Comparison of the H'...H'' distances in Figure 1 suggests that the SiH₅ transition state lies much further into the exit channel (SiH₄ + H) than does the CH₃ saddle point. This is supported by the comparison in Table I of the percent increases in the XH' and H'...H'' distances relative to the separated products (e.g., CH₄ vs. H₂). According to this picture, CH₃^{*} lies approximately in the middle of the reaction path, while SiH₅^{*} lies much closer to SiH₄ + H. Similar comparisons apply to NH₃ vs. PH₃. In fact, the PH' transition-state bond length is only 8% longer than that in PH₃. These results suggest smaller barriers to the back reaction (H + XH_n → H₂ + XH_{n-1}) in the second row relative to the first row. This is consistent with generally weaker XH bonds in the second row.² The NH₄ and PH₄ reaction paths maintain only C_s symmetry, and the XH'H'' angles bend slightly away from linear in both systems.

B. Energetics. The barriers calculated for the H + H₂ reaction are listed in Table II for a number of basis sets and computational levels. The values in the table may be compared with the 9.8-kcal/mol barrier predicted by the very accurate CI calculations of Siegbahn and Liu.³ As expected, the SCF barriers are much too high, although the UHF calculations predict substantially smaller barrier heights. For a given basis set, addition of second- and third-order perturbation corrections to the UHF wave functions successively lower the barrier. Splitting the valence sp basis set (from 6-31G to 6-311G) and adding polarization functions both reduce the barrier by about the same amount at correlated levels and the two effects appear to be approximately additive. With each basis set for which comparisons are possible, the MCSCF + POL-CI barrier is well below that predicted by the perturbation methods. Finally, it should be noted that the UHF and UMP2 results quoted in Table II are rather different from the values reported by Klimo and Tino.⁶ These authors used a minimal basis set augmented by s and p bond functions and found UHF and UMP2 barriers of 9.9 and 6.5 kcal/mol, respectively.

The energetics for the CH₃ reaction are summarized in Table III. For the forward reaction, UHF, UMP2, and UMP3 appear to be rather insensitive to basis set changes. Introduction of correlation at the MP2 level drops the barrier by about 35%, and

(16) P. Botschwina and W. Meyer, *Chem. Phys.*, 20, 43 (1977).

(17) G. C. Schatz, S. P. Walch, and A. F. Wagner, *J. Chem. Phys.*, 73, 4536 (1980).

Table IV. Energetics in the $SiH_3 + H_2 \xrightarrow{\Delta E_1} SiH_3 \xrightarrow{-\Delta E_2} SiH_4 + H$ Reaction (kcal/mol)

method	ΔE_1	ΔE_2	ΔE^a
RHF/6-31G*	26.6	21.2	-5.4
UHF/6-31G*	22.6	17.0	-5.6
UMP2/6-31G*	22.2	14.3	-7.9
UMP3/6-31G*	22.9	13.1	-9.8
MCSCF/6-31G*	27.3	21.9	-5.4
POL-CI/6-31G*	19.2	9.3	-9.9
UHF/6-31G**	23.6	16.4	-7.2
UMP2/6-31G**	22.8	11.8	-11.0
UMP3/6-31G**	23.3	10.8	-12.5

^a $\Delta E_2 - \Delta E_1$.

this drop is slightly attenuated by the introduction of third-order corrections. The MCSCF result for ΔE_1 is only slightly (1.6 kcal/mol) below that of UHF at the 6-31G* level, but the POL-CI ΔE_1 is in close agreement with the experimental estimate. The latter is somewhat misleading, since POL-CI tends to underestimate angular correlation in H_2 ,⁴ thereby raising this point relative to the other two points of interest. This will also cause the thermodynamic ΔE to be too large (see below).

For the reverse reaction, additional splitting of the valence part of the basis set and addition of polarization functions to the hydrogens both have a larger effect, with significant reductions in the barrier for UHF, UMP2, and UMP3. The latter decreases the barrier relative to second order in contrast with the forward reaction. This behavior is similar to that found for the analogous $H + H_2$ reaction, as is the lower barrier predicted by POL-CI (relative to UMP3) for a comparable basis set. All of the predicted values for ΔE_2 are well above the experimental value.⁴ All methods overestimate the experimental thermodynamic ΔE . Examination of section C of Table III reveals that the perturbation theory calculations are approaching the experimental ΔE from above as the order of the correction and size of the basis set are increased.

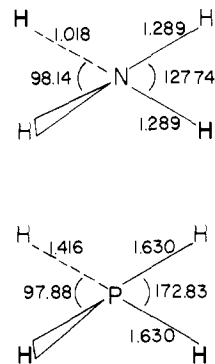
The energetics for the SiH_3 surface are summarized in Table IV. As noted for the carbon analogue, the forward reaction is virtually unaffected by basis set changes. Correlation effects are small here as well. Since ΔE_2 is simultaneously decreasing, this has a large effect on the predicted thermodynamics for the overall reaction (ΔE). For the 6-31G** basis set ΔE_1 is insensitive to correlation corrections, while ΔE_2 is not, so here again ΔE decreases by nearly a factor of 2 from UHF to UMP3.

The POL-CI/6-31G* values for ΔE_1 and ΔE_2 are 4.1 and 1.5 kcal/mol lower than those predicted by UMP3/6-31G**, and the POL-CI ΔE_2 is 6 kcal/mol above the experimental estimate.¹⁸ POL-CI predicts the overall reaction to favor $SiH_3 + H_2$ by about 10 kcal/mol. To obtain a qualitative estimate of the accuracy of the relative predictions for SiH_3 vs. CH_3 , note that the difference in the thermodynamics for the two reactions corresponds to the difference between a CH and an SiH bond energy. According to Walsh,²¹ this difference should be about 14.1 kcal/mol in favor of CH. The POL-CI and MP3 values of 17.6 and 18.6 kcal/mol, using 6-31G*, are in good agreement with experiment. If this calculated ΔE is partitioned into its contributions from the forward and reverse reactions (cf. Table III and IV), it is seen that the difference between the carbon and silicon systems arises from both ΔE_1 and ΔE_2 . In particular, the ability of SiH_3 vs. CH_3 to abstract a hydrogen from H_2 differs by 7–9 kcal/mol, whereas the barrier restricting H abstraction from SiH_4 is 8–11 kcal/mol lower than that for CH_4 .

The energetics for the $NH_2 + H_2$ and $PH_2 + H_2$ reactions are summarized in Table V. For these systems only the 6-31G* basis set was used. At this level POL-CI predicts lower barriers for both the forward and reverse NH_4 reactions than does UMP3. As a result, the two methods find $NH_3 + H$ to be lower than $NH_2 + H_2$ by about the same amount. Similar comments apply to the PH_4 system, for which the thermodynamic equilibrium is predicted to lie much closer to $PH_2 + H_2$. In the case of PH_4 , POL-CI

Table V. Energetics in the $XH_2 + H_2 \xrightarrow{\Delta E_1} XH_3 \xrightarrow{-\Delta E_2} XH_4 + H$ Reaction (kcal/mol), X = N, P

method	ΔE_1		ΔE_2		ΔE^a	
	N	P	N	P	N	P
RHF/6-31G*	31.7	32.2	32.0	16.0	0.3	-16.2
UHF/6-31G*	27.8	31.2	26.2	12.7	-1.6	-18.5
UMP2/6-31G*	15.4	28.9	25.6	10.9	10.2	-18.0
UMP3/6-31G*	19.0	30.3	23.8	10.2	4.8	-20.1
MCSCF/6-31G*	25.1	31.2	24.6	12.2	-0.5	-19.0
POL-CI/6-31G*	11.2	26.2	17.6	5.6	6.4	-19.8

^a $\Delta E_2 - \Delta E_1$.Figure 3. Structures of NH_4 and PH_4 in C_{2v} symmetry. Bond lengths in angstroms, angles in degrees.

predicts much lower barriers in both directions than do the Møller–Plesset methods. In fact, according to the POL-CI results, a barrier of only 5.6 kcal/mol prevents the abstraction of H from PH_3 .

For both the $NH_3 \cdots H$ and $PH_3 \cdots H$ systems it is of interest to determine where the XH_4 species lies on the relative energy scale and if, in fact, such species correspond to energy minima. Geometry optimization of the 3-21G tetrahedral 2A_1 structures leads to bond lengths of 1.086 and 1.630 Å, respectively, for NH_4 and PH_4 . However, both of these structures are unstable to distortions to C_{2v} and C_{3v} symmetry. The C_{2v} 2A_1 structures, shown in Figure 3, exhibit one short and one long pair of XH bonds. Both of these structures are at best metastable, however, since they are 29.4 and 5.8 kcal/mol, respectively, above the NH_4 and PH_4 abstraction transition states at the 3-21G SCF level. In C_{3v} symmetry PH_4 dissociates to $PH_3 + H$ with no barrier, while NH_4 stretches to a very long (3.09 Å) $NH_3 \cdots H$ distance. The latter structure has virtually the same energy as $NH_3 + H$, so one can conclude that stable species do not exist for NH_4 or PH_4 .

C. Normal Mode Frequencies. The 3-21G normal mode frequencies for the four sets of systems are listed in Tables VI–IX. The frequencies for NH_3 and PH_3 were taken from earlier papers,⁸ while the remaining values are obtained by using a single-point difference formula. This accounts for the slight differences relative to earlier results.²⁰ Except for the imaginary frequency, the correlations, absolute values, and most trends are in good agreement with the frequencies quoted by Schatz, Walch, and Wagner. The imaginary frequency, corresponding to the reaction path at the transition state, is a factor of 2 too high. This is consistent with the shorter C–H distance in the transition state. The analogous correlation for the SiH_3 surface is given in Table VII. As one would expect, these frequencies are generally about 30% smaller than in the carbon system, reflecting the weaker Si–H bonding and the more diffuse nature of the electron density. Two exceptions to this are the imaginary frequency, which is nearly identical in the two transition states, and the out-of-plane bend

(19) "Selected Values of Chemical Thermodynamic Properties", N. B. S. Technical Note 270-3, U. S. Government Printing Office, Washington, D. C., 1968.

(20) W. J. Pietro, M. M. Francl, W. J. Hehre, D. L. DeFrees, J. A. Pople, and J. S. Binkley, *J. Am. Chem. Soc.*, **104**, 5039 (1982).(21) R. Walsh, *Acc. Chem. Res.*, **14**, 246 (1981).(18) N. L. Arthur and T. N. Bell, *Rev. Chem. Intermed.*, **2**, 37 (1978).

Table VI. Correlation of $\text{CH}_4 + \text{H} \rightleftharpoons \text{CH}_5 \rightleftharpoons \text{CH}_3 + \text{H}_2$ Frequencies (cm^{-1})^a

vibrational motion	CH_4	CH_5^\ddagger	$\text{CH}_3 + \text{H}_2$
symmetric stretch	$\nu_1(\text{A})$: 3174 (3143)	$\nu_3(\text{A})$: 3205 (3228)	$\nu_1(\text{A})$: 3230 (3044)
asymmetric stretch	$\nu_3(\text{T})$: 3266 (3154)	$\nu_7(\text{E})$: 3336 (3404)	$\nu_3(\text{E})$: 3409 (3126)
		$\nu_2(\text{A})$: 1555 (1960)	$\nu(\text{H}_2)$: 4700 (4395)
out-of-plane bend	$\nu_4(\text{T})$: 1522 (1357)	$\nu_1(\text{A})$: 1252 (995)	$\nu_2(\text{A})$: 429 (617)
		$\nu_5(\text{E})$: 1350 (1146)	
in-plane bend	$\nu_2(\text{E})$: 1741 (1573)	$\nu_6(\text{E})$: 1604 (1534)	$\nu_4(\text{E})$: 1544 (1398)
C-H-H bend		$\nu_4(\text{E})$: 618 (592)	
C-H-H asym stretch		$\nu_1(\text{A})$: 2172i (974i)	

^a Notation taken from Table VI of ref 17. Schatz et al. frequencies in parentheses.

Table VII. Correlation of $\text{SiH}_4 + \text{H} \rightleftharpoons \text{SiH}_5 \rightleftharpoons \text{SiH}_3 + \text{H}_2$ Frequencies (cm^{-1})^a

vibrational motion	SiH_4	SiH_5^\ddagger	$\text{SiH}_3 + \text{H}_2$
symmetric stretch	$\nu_1(\text{A})$: 2287 (2377)	$\nu_3(\text{A})$: 2265	$\nu_1(\text{A})$: 2264
asymmetric stretch	$\nu_3(\text{T})$: 2277 (2319)	$\nu_7(\text{E})$: 2269	$\nu_3(\text{E})$: 2285
		$\nu_2(\text{A})$: 1056	$\nu(\text{H}_2)$: 4700 (4395)
out-of-plane bend	$\nu_4(\text{T})$: 974 (945)	$\nu_1(\text{A})$: 905	$\nu_2(\text{A})$: 779
		$\nu_5(\text{E})$: 1005	
in-plane bend	$\nu_2(\text{E})$: 1047 (975)	$\nu_6(\text{E})$: 1128	$\nu_4(\text{E})$: 988
Si-H-H bend		$\nu_4(\text{E})$: 380	
Si-H-H asym stretch		$\nu_1(\text{A})$: 1971i	

^a Notation taken from Table VI of ref 17. Harmonic frequencies (in parentheses) are taken from I. W. Levin and W. T. King, *J. Chem. Phys.*, 37, 1375 (1962).

Table VIII. Correlation of $\text{NH}_3 + \text{H} \rightleftharpoons \text{NH}_4^\ddagger \rightleftharpoons \text{NH}_2 + \text{H}_2$ Frequencies (cm^{-1})^a

vibrational motion	NH_3^b	NH_4^\ddagger	$\text{NH}_2 + \text{H}_2^b$
symmetric stretch	$\nu_1(\text{A})$: 3639 (3506)	ν_1 : 3491	$\nu_1(\text{A})$: 3381
asymmetric stretch	$\nu_3(\text{E})$: 3796 (3577)	ν_2 : 3606	$\nu_3(\text{B})$: 3485
		ν_2 : 1750	$\nu(\text{H}_2)$: 4700
symmetric bend	$\nu_2(\text{A})$: 856 (1022)	ν_4 : 1218	$\nu_2(\text{A})$: 1699
degenerate bend	$\nu_4(\text{E})$: 1858 (1691)	ν_3 : 1569	
		ν_6 : 1579	
N-H-H bend		ν_7 : 722	
		ν_8 : 730	
N-H-H asym stretch		ν_9 : 2812i	

^a Experimental harmonic frequencies in parentheses: J. L. Duncan and I. M. Mills, *Spectrochim. Acta*, 20, 523 (1964).

^b Frequency numbering system from G. Herzberg, "Infrared and Raman Spectra", G. Van Nostrand, New York, 1945.

in the product. The SiH_3 bend is found to have a larger frequency than that for CH_3 . This is apparently a result of the difference in the structures of the two radicals: strongly pyramidal in SiH_3 vs. weakly planar in CH_3 .

There are some differences of note between the two correlations in Tables VI and VII. As noted by Schatz et al.,¹⁷ the bending frequencies in the carbon case exhibit a steady decrease from reactant (CH_4) to product ($\text{CH}_3 + \text{H}_2$). In contrast, both ν_5 and ν_6 at the SiH_5 transition state are higher than either of the correlating reactant or product frequencies. Furthermore, the variation in both the symmetric and antisymmetric stretching frequencies is much smaller for silicon than for carbon. This reflects the smaller change in internal molecular structure from SiH_4 to SiH_5 to SiH_3 . In both molecules ν_2 in the transition state eventually becomes the H_2 stretch and XH_3 translational motion, while ν_5 becomes rotational and relative orbital motion in the products.

Similar correlations of normal mode frequencies for the nitrogen and phosphorus systems are presented in Tables VIII and IX, respectively. The calculated frequencies for the reactant molecules, ammonia and phosphine, are generally within 10–15% of the experimental values, and the trends relating the two molecules are correctly reproduced. This includes the larger frequency for the symmetric bending motion in phosphine. Despite the fact that the C_{3v} symmetry is destroyed during the reaction, the degenerate bending motion of XH_3 remains nearly degenerate in the XH_4 transition state for both systems. In PH_4 , for which the transition state is very close to the reactants, the bending frequencies are nearly the same as ν_4 in PH_3 . While ν_5 and ν_6 are as close to each other in NH_4^\ddagger as in PH_4^\ddagger , the decrease in magnitude relative to

Table IX. Correlation of $\text{PH}_3 + \text{H} \rightleftharpoons \text{PH}_4^\ddagger \rightleftharpoons \text{PH}_2 + \text{H}_2$ Frequencies (cm^{-1})^a

vibrational motion	PH_3^b	PH_4^\ddagger	$\text{PH}_2 + \text{H}_2^b$
symmetric stretch	$\nu_1(\text{A})$: 2404 (2452)	ν_1 : 2378	$\nu_1(\text{A})$: 2345
asymmetric stretch	$\nu_3(\text{E})$: 2398 (2457)	ν_2 : 2368	$\nu_3(\text{B})$: 2339
		ν_3 : 1219	$\nu(\text{H}_2)$: 4700
symmetric bend	$\nu_2(\text{A})$: 1093 (1041)	ν_4 : 1073	$\nu_2(\text{A})$: 1224
degenerate bend	$\nu_4(\text{E})$: 1271 (1154)	ν_5 : 1250	
		ν_6 : 1265	
P-H-H bend		ν_7 : 496	
		ν_8 : 511	
P-H-H asym stretch		ν_9 : 1783i	

^a Harmonic frequencies in parentheses: J. L. Duncan and I. M. Mills, *Spectrochim. Acta*, 20, 523 (1964). ^b Frequency numbering system from G. Herzberg, "Infrared and Raman Spectra", G. Van Nostrand, New York, 1945.

NH_3 is greater since the transition-state structure is closer to products in the nitrogen system. As noted earlier for the out-of-plane bend (ν_5) in CH_5^\ddagger and SiH_5^\ddagger , the degenerate bends become rotational and relative orbital motions of the fragments $\text{XH}_2 + \text{H}_2$.

The small deviation of the X-H-H angles from linearity in the NH_4 and PH_4 transition states has only a minor effect on the degeneracies of the corresponding frequencies. Note also that the imaginary frequency (corresponding to the X-H-H asymmetric stretch) is much larger in NH_4^\ddagger than in PH_4^\ddagger , again reflecting the very small deviation of PH_4^\ddagger from PH_3 . In view of the comparison between our CH_5^\ddagger imaginary frequency and that of Schatz and co-workers,¹⁷ it is likely that the predicted frequencies for NH_4 and PH_4 are too high. The remaining frequencies in PH_4^\ddagger also illustrate how close the PH_4^\ddagger structure is to PH_3 . In contrast, ν_1 , ν_2 , and ν_4 in NH_4^\ddagger are approximately halfway between the corresponding values in NH_3 and NH_2 .

IV. Conclusions

The principal findings of the present work, on the basis of the POL-CI/6-31G* results summarized in Figure 4, are as follows: (1) The relative abilities of CH_3 and SiH_3 to abstract hydrogens are consistent with the observed thermodynamics, which finds C-H bonds to be much stronger than Si-H bonds. Thus, CH_3 is much more able to abstract an H from H_2 . (2) The barrier resisting abstraction of H from phosphine is predicted to be very small and could vanish altogether if the entire calculation were carried out with more accurate wave functions. (3) For the prediction of abstraction barriers, the most consistent method used here appears

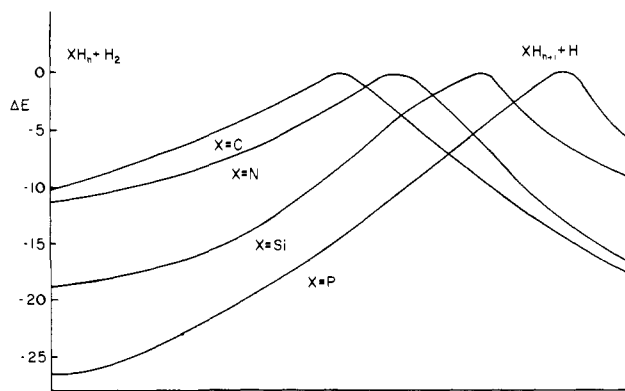


Figure 4. Schematic of POL-CI potential energy curves. The zero of energy is arbitrarily taken to be the transition state in each curve. The position of the transition state along the "reaction path" is determined by the relative bond length changes in Table I.

Table X. CPU Time Comparisons for CH_5^a

method ^b	time, ^c min	method ^b	time, ^c min
RHF/6-31G*	8	UMP3/6-311G*	28
UHF/6-31G*	4	UMP3/6-31G**	64
UMP3/6-31G*	11	UMP3/6-311G**	130
POL-CI/6-31G*	30		

^a All calculations were performed on an IBM 370/158. ^b The RHF- and UHF-based calculations were carried out with ALIS and GAUSSIAN80, respectively. ^c All times are cumulative.

to be a small MCSCF augmented by POL-CI. Thermodynamic differences, and therefore relative barriers, appear to be predicted equally well by Møller-Plesset methods.

Errors in the predicted energetics can arise from deficiencies in both the basis sets and computational levels. Since the predicted thermodynamic ΔE 's appear to be in reasonable agreement with available experimental results, it is most important to estimate errors in the POL-CI/6-31G* barriers. Walch⁴ has estimated that his value of 15.9 kcal/mol for the $\text{H} + \text{CH}_4$ barrier is close to the basis set limit for POL-CI and, using the $\text{H} + \text{H}_2$ reaction, estimates the POL-CI error to be about 2.4 kcal/mol. Since the

POL-CI/6-31G* barrier for the same reaction is 17.6 kcal/mol, one can estimate a 4.1 kcal/mol error for this level of theory, approximately equally split between basis set and methodology. If similar errors (~ 4 kcal/mol) apply to the other three systems treated here, then the $\text{H}_2 + \text{XH}_3$ barriers would be reduced to 15.2, 7.2, and 22.2 kcal/mol, respectively, for $\text{X} = \text{Si}, \text{N},$ and P . The barriers for the reverse reactions would concomitantly be reduced to 5.3, 13.6, and 1.6 kcal/mol. The latter is consistent with point 2 above.

Regarding the third point listed above, it is useful to consider Table X in which the 370/158 computer times required for the various methods are compared for CH_5 . These times are not directly comparable, since they arise from two rather different sets of codes (GAUSS80 vs. ALIS). Nonetheless, they do provide some sense for the relative times required to carry out these calculations. For the same basis set (i.e., 6-31G*) UMP3 is apparently much faster than POL-CI; however, this must be viewed in the context of the relative accuracy of the calculations. To obtain barriers at the UMP3 level which are comparable with the POL-CI results requires the use of 6-31G** or 6-311G** basis sets (cf. Tables II-IV). This makes the POL-CI approach more desirable if these comparisons hold up for more complex systems. On the other hand, it should also be noted that for transition states which do not have linear or nearly linear $\text{X}\cdots\text{H}\cdots\text{Y}$ structures, the choice of reference configurations in the MCSCF may be more complicated, and this may raise the number of configurations and time required in the POL-CI step. Finally, as noted above, UMP3 and POL-CI do predict comparable *relative* barriers at the same basis set level, and this will clearly increase in importance as the sizes of the molecules increase.

Acknowledgment. This work was supported by the donors of the Petroleum Research Fund, administered by the American Chemical Society. The computer time made available by the North Dakota State University Computer Center is gratefully acknowledged, as are very helpful discussions with Professor R. D. Koob and Mr. Clayton George. Finally, the authors are particularly grateful to Professor S. Topiol for making the IBM version of GAUSSIAN80 available and Professor K. Ruedenberg and his group for their generosity in giving us a copy of ALIS.

Registry No. CH_3 , 2229-07-4; SiH_3 , 13765-44-1; NH_2 , 13770-40-6; PH_2 , 13765-43-0; H_2 , 1333-74-0.

Experimental and Theoretical Investigations of the Unimolecular Dissociation of Nascent Ion-Molecule Clusters: $\text{H}_2\text{O}\cdot\text{H}_3\text{O}^+$, $\text{NH}_3\cdot\text{NH}_4^+$, and $\text{CO}_2\cdot\text{CO}_2^+$.

A. J. Illies, M. F. Jarrold, L. M. Bass,[†] and M. T. Bowers*

Contribution from the Department of Chemistry, University of California, Santa Barbara, California 93106. Received February 28, 1983

Abstract: The metastable fragmentation of three nascent gas-phase ion-molecule collision complexes, $\text{H}_2\text{O}\cdot\text{H}_3\text{O}^+$, $\text{NH}_3\cdot\text{NH}_4^+$, and $\text{CO}_2\cdot\text{CO}_2^+$, has been studied using mass-analyzed ion kinetic energy spectrometry (MIKES). The clusters were formed in an ion source which was cooled to promote the association reactions. The kinetic energy release distributions and the metastable intensities were measured as a function of the ion source pressure. The metastable fragmentation was modeled using statistical phase space theory. The experimental data and theoretical results suggest that a single collision between the nascent cluster and a molecule is sufficient to quench the unimolecular reaction.

I. Introduction

Studies of proton-bound dimers and ionic clusters by high-pressure mass spectrometry and ion cyclotron resonance spec-

trometry have resulted in a thorough understanding of the thermodynamics and kinetics of formation for many ion-molecule clusters.¹⁻⁵ The motive behind the intense research in this area

[†] Present Address: Department of Chemistry, University of Warwick, Coventry, CV4 7AL, UK.

(1) P. Kebarle, *Annu. Rev. Phys. Chem.*, **28**, 445 (1977).
(2) M. Meot-Ner in "Gas Phase Ion Chemistry", Vol. 1, M. T. Bowers, Ed., Academic Press, New York, 1979.